JOURNAL OF GEOPHYSICAL RESEARCH, VOL. 100, NO. B11, PAGES 22,375–22,381, NOVEMBER 10, 1995

Stoneley and flexural modes in pressurized boreholes

Bikash K. Sinha and Sergio Kostek
Schlumberger-Doll Research, Ridgefield, Connecticut

Andrew N. Norris
Department of Mechanical and Aerospace Engineering, Rutgers University, Piscataway, New Jersey

Abstract. The propagation of Stoneley and flexural waves in a fluid-filled borehole is adequately described by the linear equations of elasticity. However, when the borehole fluid is pressurized either due to the hydrostatic head at a given depth or with the aid of packers at the wellhead, both the fluid and the surrounding formation are subjected to biasing stresses. Under this situation, wave propagation along the borehole is described by the equations of motion for small dynamic fields superposed on a bias. The resulting formulation allows us to study the influence of a change in the fluid pressure on the Stoneley and flexural mode dispersion curves. Since the biasing stresses in the surrounding formation exhibit a radial decay away from the borehole, it is expedient to employ a perturbation technique to calculate changes in the borehole Stoneley and flexural wave dispersion curves as a function of hydrostatic pressure change in the fluid. A key advantage of this perturbation technique is that it separates contributions of the acoustoelastic effect due to the borehole fluid and that due to the formation. Insofar as the fluid nonlinear properties at a given pressure and temperature are known, the model provides a procedure for estimating the acoustoelastic coefficient of the formation for the borehole Stoneley and flexural wave velocities for a given change in the fluid pressure. The formation acoustoelastic coefficient can be expressed as a fractional change in the acoustic wave velocity caused by a unit change in the borehole pressure. Computational results show that acoustoelastic coefficients for the Stoneley and flexural waves are larger for formations with higher degree of nonlinearity which is typically associated with poorly consolidated rocks.

Introduction

Nonlinear effects in rocks are seen in two instances: (1) finite amplitude elastic wave propagation resulting in harmonic generation and frequency mixing; and (2) stress dependence of acoustic wave velocities. Finite amplitude effects have recently been studied by *Johnson et al.* [1987], *Johnson and Shankland* [1989], *Johnson et al.* [1991], and *Meegan et al.* [1993] in rocks and by *Johnson et al.* [1994] in a borehole environment. Microscopically, nonlinearity of rocks expressed as a nonlinear relationship between stresses and strains may be caused by several sources, such as intrinsic nonlinear behavior of the formation; crack closure and dilatancy in a fractured formation; and nonlinear deformation of a granular medium subject to an externally applied load. Macroscopically, we can express the nonlinearity of the formation implicitly in terms of the third-order elastic constants independent of the source of nonlinearity. The nonlinear third-order elastic constants of a medium essentially provide a measure of changes in the effective elastic stiffnesses as a function of externally applied strain. For instance, when cracks in a fractured medium close due to an increase in the confining pressure, its effective stiffnesses increase and the third-order elastic constants, generally, attain negative values that results in an increase in the acoustic wave velocity. On the other hand, increasing applied stresses may also cause dilatancy and failure in the rock, resulting in a decrease in the effective elastic stiffnesses. In this situation, the third-order elastic constants, generally, attain positive values that results in a decrease in the acoustic wave velocity. The magnitudes of third-order elastic constants are functions of stresses in the reference state. The algebraic signs of these constants may be either positive or negative.

The effective elastic stiffnesses, mass density, and path length between two observation points change when the propagating medium is statically deformed, resulting in a corresponding change in the acoustic wave velocity. The dependence of the acoustic wave velocity on biasing stresses in the propagating medium is referred to as the acoustoelastic phenomenon [*Hughes and Kelly*, 1953; *Toupin and Bernstein*, 1961; *Thurston and Brugger*, 1964]. While stress-induced effects in rocks have been long recognized and studied under laboratory conditions [see *Johnson et al.*, 1994, and references therein], these effects on borehole waves have received little attention.

In this paper we present a study of the nonlinear effects on the wave speeds of borehole modes due to a prestressed state caused by the pressurization of the borehole. We note that the pressurization of the borehole can be caused by the hydrostatic head of the borehole fluid at a given depth and further increased with the help of packers at the wellhead. In particular, we study these stress effects on Stoneley and flexural modes, thus giving a direct way to detect acoustoelastic behavior of the formation surrounding the borehole. Acoustoelastic coefficients for the formation can be expressed as a fractional change in the Stoneley or flexural wave velocities caused by a

Paper number 95JB02504.
0148-0227/95/95JB-02504$05.00

known increase in the borehole pressure. The formation acoustoelastic coefficient depends on its linear as well as nonlinear constants defined about a reference state. While a definite correlation between the acoustoelastic coefficients and mechanical strength remains to be established, there is some laboratory evidence linking the stress induced nonlinearity of the material to its mechanical strengths [*Shkolnik et al.*, 1990; K. W. Winkler, private communication, 1993]. In addition, poorly consolidated rocks with higher compressional to shear velocity (v_P/v_S) ratio, generally, exhibit a higher degree of nonlinearity. A higher degree of material nonlinearity results in larger acoustoelastic coefficients for acoustic wave velocities. Potential applications of formation nonlinearity are in the prediction of sanding and borehole breakouts in the presence of tectonic stresses and design of hydraulic fracturing for enhanced recovery through an improved understanding of its mechanical properties.

Theory

The propagation of small-amplitude waves in an isotropic and homogeneous medium is governed by the linear equations of motion. However, when the propagating medium is prestressed, the propagation of such waves are properly described by equations of motion for small dynamic fields superposed on a static bias [*Sinha and Tiersten*, 1979; *Sinha*, 1982]. A static bias represents any statically deformed state of the medium due to an externally applied load or residual stresses. The equations of motion for small dynamic fields superposed on a static bias are derived from the rotationally invariant equations of nonlinear elasticity by making a Taylor expansion of the quantities for the dynamic state about their values in the biasing (or intermediate) state.

When the biasing state is inhomogeneous, the effective elastic constants are position dependent, and a direct solution of the boundary value problem is not possible. Under this situation, a perturbation procedure [*Tiersten*, 1978; *Sinha and Tiersten*, 1979; *Norris et al.*, 1994] can readily treat spatially varying biasing states, such as those due to a nonuniform radial stress distribution away from the borehole, and the corresponding changes in the Stoneley and flexural wave velocities can be calculated as a function of frequency. Referred to the statically deformed state of the pressurized borehole (or the intermediate configuration), we employ the modified Piola-Kirchhoff stress tensor $P_{\alpha j}$ as defined by *Norris et al.* [1994] in a perturbation model that yields the following expression for the first-order perturbation in the eigenfrequency ω_m for a given wavenumber k_z:

$$\Delta\omega = \frac{\int_V \Delta P_{\alpha j} u^m_{j,\alpha}\, dV - \omega_m^2 \int_V \Delta\rho u^m_j u^m_j\, dV}{2\omega_m \int_V \rho_0 u^m_j u^m_j\, dV}, \tag{1}$$

where

$$\Delta P_{\alpha j} = H_{\alpha j\gamma\beta} u^m_{\gamma,\beta}, \tag{2}$$

$$H_{\alpha j\gamma\beta} = h_{\alpha j\gamma\beta} + T_{\alpha\beta}\delta_{j\gamma} + P_0(\delta_{\alpha j}\delta_{\gamma\beta} - \delta_{\alpha\gamma}\delta_{j\beta}), \tag{3}$$

$$h_{\alpha j\gamma\beta} = -c_{\alpha j\gamma\beta} w_{\delta,\delta} + c_{\alpha j\gamma\beta AB} E_{AB} + w_{\alpha,L} c_{Lj\gamma\beta} + w_{j,M} c_{\alpha M\gamma\beta} + w_{\gamma,P} c_{\alpha jP\beta} + w_{\beta,Q} c_{\alpha j\gamma Q}, \tag{4}$$

$$T_{\alpha\beta} = c_{\alpha\beta\gamma\delta} w_{\delta,\gamma}, \tag{5}$$

$$E_{AB} = \tfrac{1}{2}(w_{A,B} + w_{B,A}). \tag{6}$$

In (1)–(6), we have used the Cartesian tensor notation and the convention that a comma followed by an index P denotes differentiation with respect to X_P. The summation convention for repeated tensor indices is also implied. Although $h_{\alpha j\gamma\beta}$ exhibits the usual symmetries of the second-order constants of linear elasticity, the effective elastic stiffness tensor $H_{\alpha j\gamma\beta}$ does not have these properties as it is evident from (3).

Before discussing the various quantities in (1)–(6), we note that the present position of material points may be written as

$$\mathbf{y}(\mathbf{X}, t) = \mathbf{X} + \mathbf{w}(\mathbf{X}) + \mathbf{u}(\mathbf{X}, t), \tag{7}$$

where $\mathbf{w}$ denotes the displacement due to the applied static loading of material points with position vector $\mathbf{X}$ in the reference state and $\mathbf{u}$ denotes the small dynamic displacement vector of material points above and beyond that due to the static deformation. The "small-on-large" theory is based on the assumption that $|\mathbf{u}| \ll |\mathbf{w}|$ and that the associated deformation gradients are similarly related, $|\partial\mathbf{u}/\partial\mathbf{X}| \ll |\partial\mathbf{w}/\partial\mathbf{X}|$. These assumptions are, generally, valid when one deals with static deformations of the order of millistrain measured from a reference state and dynamic deformations associated with the acoustic waves on the order of microstrain measured from the statically deformed state. However, the total displacement gradient of a material point from the reference state must also satisfy the condition $|\partial\mathbf{u}/\partial\mathbf{X}| + |\partial\mathbf{w}/\partial\mathbf{X}| \ll 1$. This requires that the reference state must be selected relatively close to the current state of stress in the formation for the third-order elasticity theory to be valid. The small field Piola-Kirchhoff stress $P_{\alpha j}$ in the intermediate state can be decomposed into two parts

$$P_{\alpha j} = P^{\mathrm{L}}_{\alpha j} + \Delta P_{\alpha j}, \tag{8}$$

where

$$P^{\mathrm{L}}_{\alpha j} = c_{\alpha j\gamma\beta} u^m_{\beta,\gamma}, \tag{9}$$

where $\Delta P_{\alpha j}$ being defined by (2)–(6) and the superscript L denotes the linear portion of the stress tensor. The quantities $c_{\alpha j\gamma\beta}$ and $c_{\alpha j\gamma\beta AB}$ are the second- and third-order elastic constants, respectively. In (3)–(6), $T_{\alpha\beta}$, E_{AB}, and $w_{\delta,\gamma}$ denote the biasing stresses, strains, and (static) displacement gradients, respectively. The quantity P_0 denotes the increase in the borehole pressure.

In (1), $\Delta P_{\alpha j}$ are the perturbations in the Piola-Kirchhoff stress tensor elements from the linear portion, $P^{\mathrm{L}}_{\alpha j}$, for the reference isotropic medium before the application of any biasing stresses; $\Delta\rho = \rho - \rho_0$, ρ and ρ_0 denote the mass density of the propagating medium in the statically deformed and reference states, respectively; and u^m_j represents the eigensolution for the reference isotropic medium for a selected propagating mode. The index m refers to a family of normal modes for a borehole in an isotropic formation. The frequency perturbations $\Delta\omega$ are added to the eigenfrequency ω_m for various values of the wavenumber along the borehole axis, k_z, to obtain the final dispersion curves for the biased state. Thus the modal solution is obtained. Although this method of solution is valid for all modes, we present in this paper results for only the Stoneley ($m = 0$) and flexural ($m = 1$) modes.

An important feature of the perturbation equation (1) is that

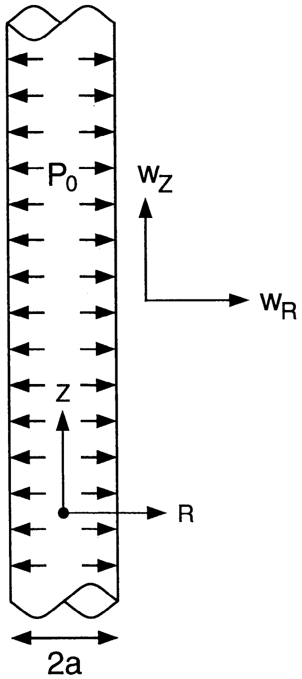

Figure 1. Schematic diagram of a pressurized borehole of radius a. The radial and axial biasing displacement components in the formation are w_R and w_Z, respectively.

the volume integral in the numerator can be separated into two independent contributions coming from the borehole fluid and formation. This has the advantage of subtracting the borehole fluid induced velocity change from the total velocity change and obtaining the acoustoelastic response of the formation which is of primary interest in this study. The volume integrals as shown in (1) are computed in the statically deformed configuration of the borehole.

Computational Results

Computational results have been obtained for the Stoneley and flexural wave dispersion curves before and after pressurization of a fluid-filled borehole surrounded by an initially isotropic nonlinear formation. Figure 1 shows a schematic diagram of a borehole of radius a, taken here as 10.16 cm (4 inches). We consider two distinct formations whose material properties are listed in Table 1. Formation 1 is a fast formation, whereas formation 2 is a moderately slow one. The nonlinearity parameter defined as $\beta = (3c_{11} + c_{111})/2c_{11}$ is substantially different for the two formations considered here. This nonlinearity parameter for rocks varies by several orders of magnitude depending on the rock type, porosity, and degree of compaction, etc. [*Johnson and McCall*, 1994], and it is substantially larger than those for nongranular materials [*Johnson et al.*, 1994].

The borehole fluid is assumed to have a compressional wave speed of 1500 m/s, and mass density $\rho_0^{\mathrm{f}} = 1000$ kg/m^3. The nonlinear behavior of the fluid is usually expressed in terms of the parameters A and B appearing in the adiabatic equation of state, $p = p_0 + A\Delta\rho/\rho_0 + B(\Delta\rho)^2/2\rho_0^2$. Here $\Delta\rho = \rho - \rho_0$, where p and ρ are the current pressure and density, respectively, with p_0 and ρ_0 being their reference values. The change in the fluid bulk modulus ΔA, caused by a change in the fluid pressure Δp can be expressed in terms of the fluid nonlinearity B/A as $\Delta A = (1 + B/A)\Delta p$. The corresponding change in the fluid mass density is simply given by $\Delta\rho = \rho_0\Delta p/A$. We take $B/A = 5$ for water and according to *Kostek et al.* [1993], the corresponding third-order elastic constants are given by $c_{111}^{\mathrm{f}} = -22.5$ GPa, $c_{112}^{\mathrm{f}} = -13.5$ GPa, and $c_{123}^{\mathrm{f}} = -9.0$ GPa.

When the borehole pressure is increased by $\Delta p = P_0$, static deformations of the borehole fluid and formation are governed by the static equations of equilibrium and continuity of radial component of particle displacement and radial stress at the borehole wall. The static deformation of the surrounding formation yields the following biasing displacements, stresses, and strains [*White*, 1983]:

$$w_R = P_0 a^2/2c_{66}R, \qquad w_Z = 0, \tag{10}$$

$$T_{RR} = -P_0 a^2/R^2, \qquad T_{\theta\theta} = P_0 a^2/R^2, \qquad T_{ZZ} = 0, \tag{11}$$

$$E_{RR} = -P_0 a^2/2c_{66}R^2, \qquad E_{\theta\theta} = P_0 a^2/2c_{66}R^2, \qquad E_{ZZ} = 0, \tag{12}$$

where w_R is the static radial displacement in the formation ($R > a$) caused by a borehole fluid pressure P_0; and c_{66} ($= \mu$) is the formation isotropic shear modulus. These expressions for the biasing stresses and strains in the formation satisfy the static equations of equilibrium in the presence of a borehole fluid pressure of P_0 under the assumption of either plane stress or plane strain. Figure 2 displays the radial and hoop stress distributions away from the borehole. Both these stresses exhibit R^{-2} dependence implying that formation stresses will have less influence on the Stoneley and flexural waves at low frequencies.

The volume integrals in (1) extend over both the borehole fluid and the solid formation. However, the fluid contribution to the first-order perturbation in the eigenfrequency ω_m can be readily computed from the expression

$$\Delta\omega_{\mathrm{fluid}} = \frac{\int_{V_{\mathrm{f}}} c^{\mathrm{f}}_{\alpha\beta\gamma\delta} u^m_{\delta,\gamma} u^m_{\beta,\alpha}\, dV - \omega_m^2 \int_{V_{\mathrm{f}}} \Delta\rho^{\mathrm{f}} u^m_\gamma u^m_\gamma\, dV}{2\omega_m \int_V \rho_0 u^m_j u^m_j\, dV}, \tag{13}$$

where

$$\Delta c^{\mathrm{f}}_{\alpha\beta\gamma\delta} = \frac{\partial A}{\partial p} P_0 \delta_{\alpha\beta}\delta_{\gamma\delta} = \left(1 + \frac{B}{A}\right) P_0 \delta_{\alpha\beta}\delta_{\gamma\delta}, \tag{14}$$

$$\Delta\rho^{\mathrm{f}} = \frac{\rho^{\mathrm{f}}}{A} P_0, \tag{15}$$

Table 1. Material Properties for Formations 1 and 2

Formation	c_{11}, GPa	c_{66}, GPa	ρ_0, kg/m^3	v_p, m/s	v_s, m/s	c_{111}, GPa	c_{112}, GPa	c_{123}, GPa	β
1	19.5	6.50	2135	3022	1745	−3,467	−1155	−1541	−87
2	11.1	4.64	2062	2320	1500	−21,217	−3044	2361	−954

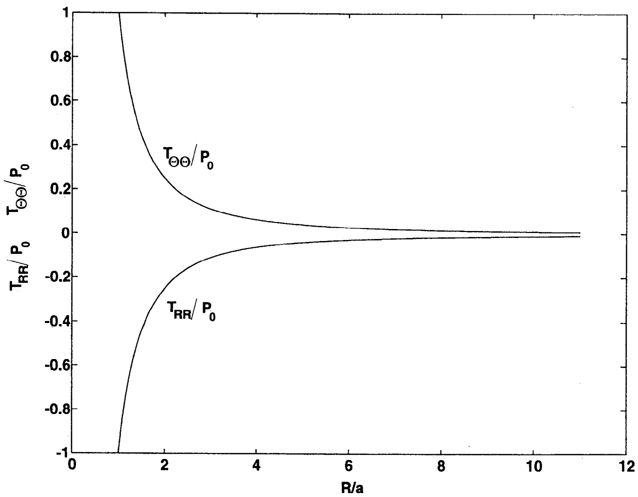

Figure 2. Radial and hoop stress distribution around a pressurized borehole.

and ρ_0^f is the mass density of the fluid in the reference state, B is the fluid nonlinear parameter appearing in the equation of state [*Kostek et al.*, 1993], and V_f denotes the fluid volume. The fractional change in phase velocity resulting from changes in effective stiffness and mass density of the material takes the form

$$\Delta v / v = \Delta\omega / \omega_m, \tag{16}$$

for a fixed wavenumber.

Stoneley Mode

In Figure 3 we show the Stoneley wave dispersion curves in formation 1 before and after the pressurization (solid lines) for $P_0 = 13.8$ MPa (2000 psi). The dashed curve denotes the contribution of the borehole fluid to the total velocity change. Notice that in the low-frequency limit the change in the tube wave speed after pressurization is essentially due to the acoustoelastic effect of the borehole fluid.

An asymptotic analysis ($\omega \rightarrow 0$) for the fractional change in the tube wave speed in a pressurized borehole leads to [*Norris et al.*, 1994]

$$\frac{\Delta v_T}{v_T} = \frac{P_0}{A}\frac{\rho^f}{v_T}\frac{\partial v_T}{\partial \rho^f} + \frac{P_0}{v_T}\left(1 + \frac{B}{A}\right)\frac{\partial v_T}{\partial A} + \frac{\displaystyle\int_{V_s} H_{\alpha j \gamma \beta} u^m_{\gamma,\beta} u^m_{j,\alpha}\, dV}{2\omega_m^2 \displaystyle\int_V \rho_0 u_j^m u_j^m\, dV}$$

$$- \frac{\displaystyle\int_{V_s} \Delta\rho u_j^m u_j^m\, dV}{2\displaystyle\int_V \rho_0 u_j^m u_j^m\, dV}, \tag{17}$$

where V_s denotes the solid volume, and the unperturbed tube wave speed v_T is given by

$$v_T^{-2} = \rho_0^f\left(\frac{1}{A} + N_1\right), \tag{18}$$

and $N_1 = 1/\mu$ for an isotropic formation of shear modulus μ [*White*, 1983]. In (17), the quantity $\Delta\rho$ in the solid formation vanishes because the deformation of the solid due to the pressurization of the borehole is a pure shear (equivoluminal). Combining this with the quasi-static approximation for the tube wave gives the following expression for the fractional change in the tube wave speed:

$$\frac{\Delta v_T}{v_T} = \frac{P_0}{2A(1 + AN_1)}\left(\frac{B}{A} - AN_1 - \tfrac{1}{2}A^2N_1^2\right). \tag{19}$$

Note that the velocity in (19) depends upon the applied pressure P_0 but not on the specific fluid strain field. This is physically reasonable and it has been previously obtained by *Johnson et al.* [1994] and *Norris et al.* [1994].

Substituting the numerical values for the quantities corresponding to formation 1 in (19), we find that $(\Delta v_T/v_T)_{\text{fluid}} =$

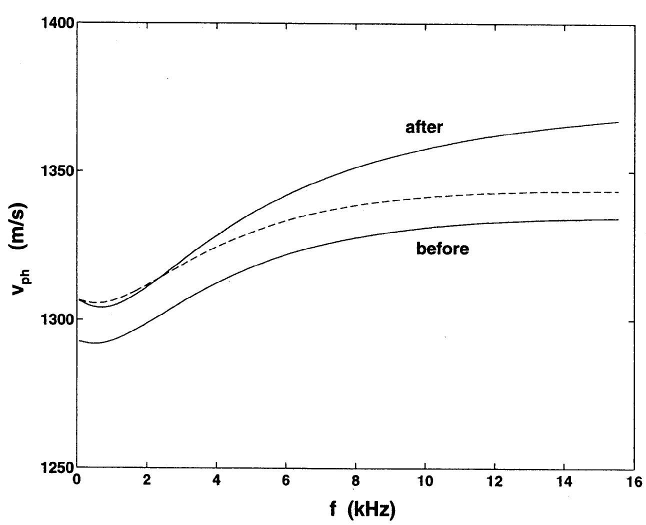

Figure 3. Dispersion curves for Stoneley waves in formation 1 before and after pressurization. The dashed curve shows the fluid contribution to the total velocity change.

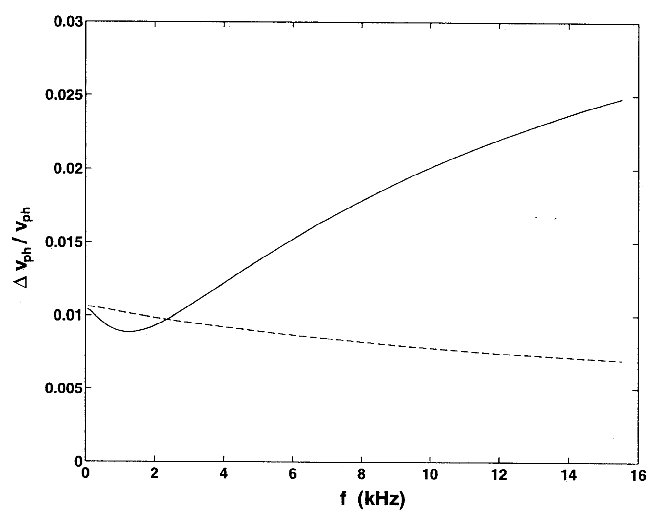

Figure 4. Fractional velocity changes for the Stoneley wave in formation 1. The solid curve represents the total change after pressurization. The dashed curve shows only the fluid contribution.

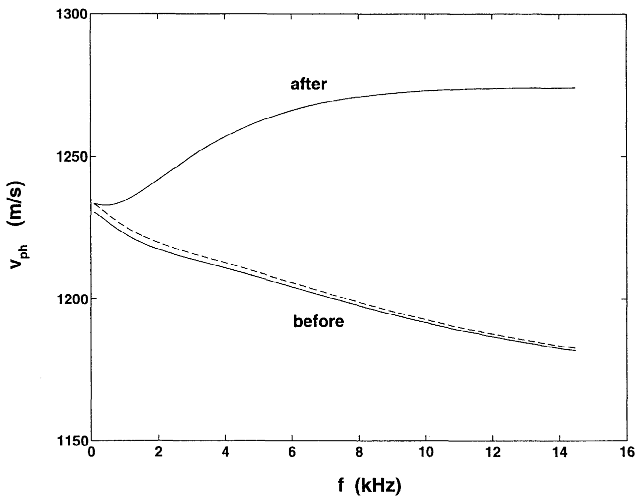

Figure 5. Dispersion curves for Stoneley waves in formation 2 before and after pressurization. The dashed curve shows the fluid contribution to the total velocity change.

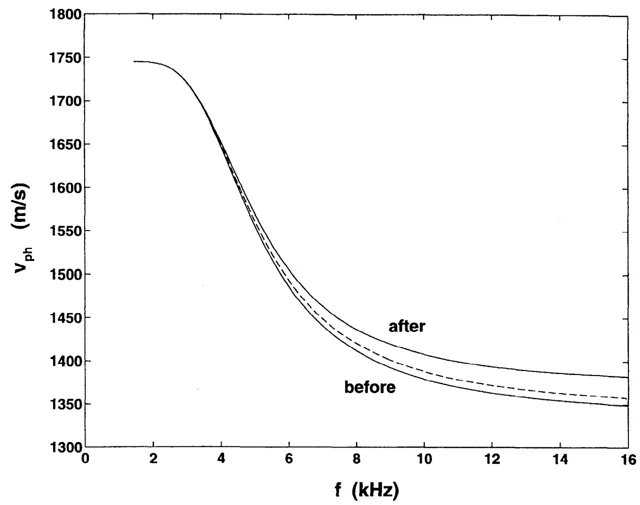

Figure 7. Dispersion curves for flexural waves in formation 1 before and after pressurization. The dashed curve shows the fluid contribution to the total velocity change.

1.05%, which is in excellent agreement with our numerical calculations in the limiting case of $\omega \to 0$. Figure 4 illustrates the fractional change in the Stoneley wave phase velocity as a function of frequency for formation 1. As expected from the stress distribution shown in Figure 2, $\Delta v/v$ increases with frequency because the acoustic field becomes more confined to the borehole wall. However, the acoustoelastic contribution from the borehole fluid decreases with increasing frequency as shown by the dashed curve. To compare the acoustoelastic coefficients for different formations, it is straightforward to divide the fractional change in the Stoneley wave velocity by the borehole pressure change P_0 = 13.8 MPa at various frequencies.

In Figures 5 and 6, we show the Stoneley wave dispersions and the fractional changes in wave speeds for formation 2, respectively. The rock parameters for this formation correspond to those of a dry Berea sandstone (K. W. Winkler, private communication, 1993). Since this formation exhibits a higher nonlinearity than formation 1, even for $P_0 = 3.4$ MPa (500 psi), we observe significant changes in the Stoneley wave speed. The dispersion characteristics of this formation before pressurization are significantly different from those of formation 1 (fast formation). The sharp increase in the Stoneley wave speed at all frequencies for formation 2 results from the high nonlinearity of the rock, and the resulting dispersion resembles that of a fast formation. Notice that the fluid contribution is swamped by the high nonlinearity of the formation. The fractional change in the Stoneley wave speed is significantly higher than in formation 1. At 4 kHz, the change is approximately 4% for 3.4 MPa (500 psi) increase in borehole pressure. Note that the fractional change in the Stoneley wave speed caused by a 3.4-MPa increase in borehole pressure for the formation 1 with significantly smaller nonlinearity turns out to be one-fourth of the values shown in Figure 4 and is deemed to be negligibly small over the moderate frequency range of interest.

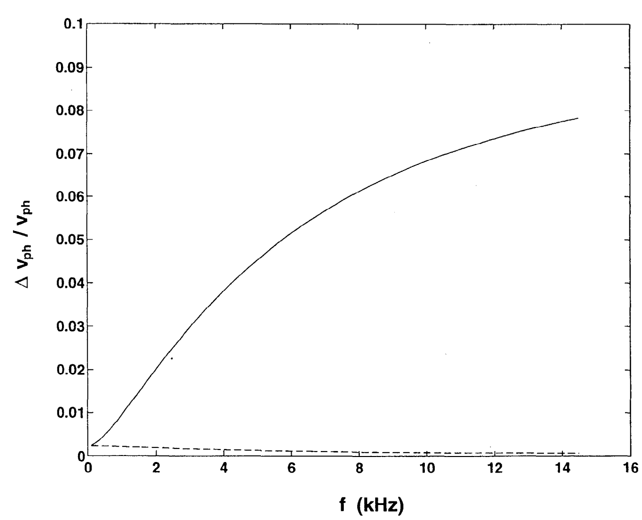

Figure 6. Fractional velocity changes for the Stoneley wave in formation 2. The solid curve represents the total change after pressurization. The dashed curve shows only the fluid contribution.

Flexural Mode

In Figure 7 we show the flexural wave dispersion curves in formation 1 before and after the pressurization for $P_0 = 13.8$ MPa (2000 psi). The contribution of the borehole fluid is shown as a dashed curve. As expected, the borehole pressure induced velocity change at low frequencies is negligibly small since the static stress field decays away from the borehole thus not changing the effective stiffness of the virgin formation which is probed by the flexural wave. At higher frequencies, both the borehole fluid and formation contribute to the total increase in velocity by approximately the same amount. The solid curve in Figure 8 illustrates the fractional change in the flexural wave velocity as a function of frequency, whereas the dashed curve denotes the borehole fluid contribution to the total $\Delta v/v$.

Figures 9 and 10 show the flexural wave dispersions and the fractional changes in wave speeds for formation 2, respectively. Similar to the Stoneley wave analysis we take $P_0 = 3.4$ MPa (500 psi). The fluid contribution is negligibly small due to the relatively low nonlinearity of the fluid when compared to that of the rock. The results are qualitatively the same as those

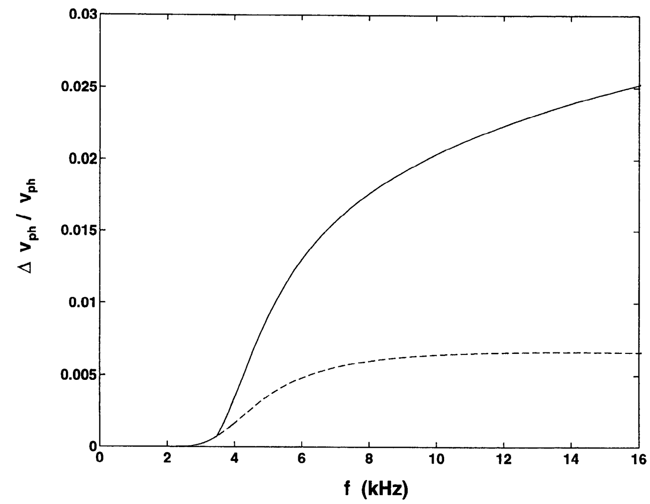

Figure 8. Fractional velocity changes for the flexural wave in formation 1. The solid curve represents the total change after pressurization. The dashed curve shows only the fluid contribution.

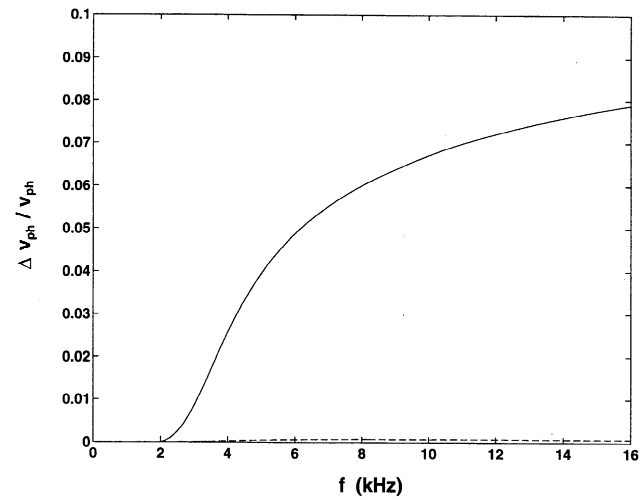

Figure 10. Fractional velocity changes for the flexural wave in formation 2. The solid curve represents the total change after pressurization. The dashed curve shows only the fluid contribution.

obtained with formation 1. However, the magnitude of the wave speed changes are considerably higher and comparable to the changes in the Stoneley wave speed at similar frequencies. For instance, at 6 kHz the fractional change in the flexural wave speed is approximately 5%. To compare the acoustoelastic coefficients for the two formations, it is straightforward to divide the fractional change in the flexural wave speed by the change in the borehole pressure at various frequencies.

Conclusions

We have developed a perturbation model to study the velocity changes in borehole Stoneley and flexural modes which incorporates nonlinear contributions due to biasing stresses, in particular, the effects of a static increase in the borehole pressure. We have shown that at low frequencies, stress-induced

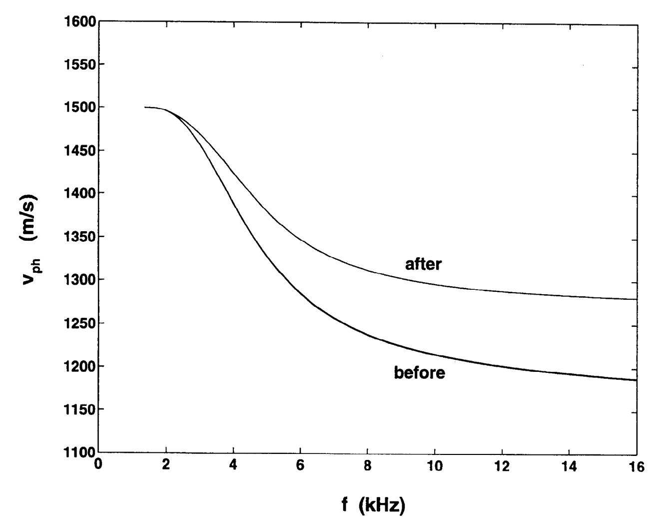

Figure 9. Dispersion curves for flexural waves in formation 2 before and after pressurization. The dashed curve showing the fluid contribution to the total velocity change is indistinguishable from the solid dispersion curve before pressurization.

Stoneley wave velocity change is basically controlled by the borehole fluid but at higher frequencies there is a significant contribution from the formation. On the other hand, while the flexural wave velocity is essentially independent of the borehole pressure at low frequencies, it increases with an increase in the borehole pressure at higher frequencies. An important aspect of this model is that it allows us to separate the contributions of the borehole fluid to the total change in modal wave speed at any frequency. Therefore, by running acoustic logs before and after pressurization we can get a direct measure of the formation acoustoelastic coefficient as a function of frequency. This coefficient can be readily obtained from the differences between the Stoneley and flexural wave velocities for a unit increase in the borehole pressure. It should be noted that the formation acoustoelastic coefficients for the Stoneley and flexural waves are estimated with respect to the ambient borehole pressure. Consequently, these coefficients provide additional information about the mechanical properties of the formation in the presence of the ambient borehole pressure. The wave speed changes that we report in this paper are obviously dependent on the magnitude of acoustoelastic coefficients of the formation and increase in borehole pressure from a reference state. The parameters that we have used are typical of some consolidated rocks, but there is evidence that they could be much higher for weaker rocks.

Practical applications of this work are in the estimation of nonlinear mechanical properties of formations through a direct measurement of acoustoelastic coefficients of the Stoneley and flexural wave velocities as a function of frequency. Poorly consolidated sandstones exhibit higher degree of nonlinearity resulting in larger magnitude of acoustoelastic coefficients. It is also concievable that a more complete characterization of the mechanical properties of formations that includes their nonlinear behavior would help in an improved prediction of sanding and borehole breakouts in the presence of tectonic stresses; and design of hydraulic fracturing of rocks for enhanced recovery. On the other hand, in the linear interpretation of the Stoneley and flexural dispersions in the presence of ambient borehole fluid pressure, the present analysis may be employed to subtract the borehole pressure induced contribution to the measured dispersions when deemed necessary.

Acknowledgments. We would like to thank K. W. Winkler for providing us with the experimental data for formation 2 and D. L. Johnson and T. J. Plona for their continuing interest in this work and fruitful discussions.

References

Hughes, D. S., and J. L. Kelly, Second-order elastic deformation of solids, *Phys. Rev.*, *92*, 1145–1149, 1953.

Johnson, D. L., S. Kostek, and A. N. Norris, Nonlinear tube waves, *J. Acoust. Soc. Am.*, *96*, 1829–1843, 1994.

Johnson, P. A., and K. R. McCall, Observation and implications of nonlinear elastic wave response in rock, *Geophys. Res. Lett.*, *21*, 165–168, 1994.

Johnson, P. A., and T. J. Shankland, Nonlinear generation of elastic waves in granite and sandstone: Continuous wave and travel time observations, *J. Geophys. Res.*, *94*, 17,729–17,733, 1989.

Johnson, P. A., T. J. Shankland, R. J. O'Connell, and J. N. Albright, Nonlinear generation of elastic waves in crystalline rocks, *J. Geophys. Res.*, *92*, 3597–3602, 1987.

Johnson, P. A., A. Migliori, and T. J. Shankland, Continuous wave phase detection for probing nonlinear elastic wave interactions in rocks, *J. Acoust. Soc. Am.*, *89*, 598–603, 1991.

Kostek, S., B. K. Sinha, and A. N. Norris, Third-order elastic constants for an inviscid fluid, *J. Acoust. Soc. Am.*, *94*, 3014–3017, 1993.

Meegan, G. D., P. A. Johnson, R. A. Guyer, and K. R. McCall, Observations of nonlinear elastic wave behaviour in sandstone, *J. Acoust. Soc. Am.*, *94*, 3387–3391, 1993.

Norris, A. N., B. K. Sinha, and S. Kostek, Acoustoelasticity of solid/fluid composite systems, *Geophys. J. Int.*, *118*, 439–446, 1994.

Shkolnik, I. E., L. K. Zarembo, and V. A. Krasilnikov, On structural non-linear diagnostics of solids and estimation of their strength, in *Frontiers of Nonlinear Acoustics: Proceedings of 12th ISNA*, edited by M. F. Hamilton, J. Wu, and T. C. T. Ting, pp. 589–594, Elsevier Sci., New York, 1990.

Sinha, B. K., Elastic waves in crystals under a bias, *Ferroelectrics*, *41*, 61–73, 1982.

Sinha, B. K., and H. F. Tiersten, On the influence of a flexural biasing state on the velocity of piezoelectric surface waves, *Wave Motion*, *1*, 37–51, 1979.

Sinha, B. K., A. N. Norris, and S. K. Chang, Borehole flexural modes in anisotropic formations, *Geophysics*, *59*, 1037–1052, 1994.

Thurston, R. N., and K. Brugger, Third-order elastic constants and the velocity of small amplitude elastic waves in homogeneously stressed media, *Phys. Rev. A*, *133*, 1604–1610, 1964.

Tiersten, H. F., Perturbation theory for linear electroelastic equations for small fields superposed on a bias, *J. Acoust. Soc. Am.*, *64*, 832–837, 1978.

Toupin, R. A., and B. Bernstein, Sound waves in deformed perfectly elastic materials. Acoustoelastic effect, *J. Acoust. Soc. Am.*, *33*, 216–225, 1961.

White, J. E., *Underground Sound*, Elsevier Sci., New York, 1983.

S. Kostek and B. K. Sinha, Schlumberger-Doll Research, Old Quarry Road, Ridgefield, CT 06877-4108. (e-mail: sinha@ridgefield, sdr.slb.com)

A. N. Norris, Department of Mechanical and Aerospace Engineering, Rutgers University, Piscataway, NJ 08855-0909.

(Received March 24, 1995; revised August 4, 1995; accepted August 10, 1995.)